Original scientific paper

Machinability behavior of human implant materials

Gurbhej Singh✉, Rajbir Singh and Jameel Gul

Amritsar Group of Colleges Amritsar, 143001, Punjab, India

Corresponding authorc: ✉*gurbhejsingh612@gmail.com*

Abstract

In this day and age, engineered materials are making significant strides in their application in the biomedical sector. Human implants have piqued the interest of material and metallurgy researchers due to their unique properties. Machining the materials into implants customized for individual patients has been the standard practice nowadays. To contribute further to the same area, the current research work aims to investigate the machinability of T-L107.12 (a titanium-based human implant) using a non-traditional method called wire electrical discharge machining (WEDM). The machinability of the machining process has been evaluated based on the material removal rate using a roughness meter and the atomic force microscope. The further impact of the machining parameters on the output responses was analyzed based on the statistical analysis.

Keywords
Titanium; roughness; material removal rate; wear

Introduction

The use of biocompatible metals in medical implants at the time of the Industrial Revolution in the 19th century led to a period that saw the beginning aspects of the process of the metal industry [1]. The key element that spurred the rise of the metal implant business was the growing need for surgical treatments to repair broken bones [2]. These operations often include the internal healing of long bone fractures. However, until the aseptic method of Lister's surgery was used in the 1860s, there were so few successes in attempts to implant metal appliances like bone pins and spinal wires composed of gold, silver, or iron [3]. These attempts were met with extremely limited levels of success. Up until recently, there were relatively few obstacles that needed to be overcome in order to implant metal appliances. After that, biocompatible metals led to the development of orthopedic applications that currently play an important role in orthopedic appliances [4-6]. These orthopedic appliances include temporary appliances like bone plates and pins and screws and permanent implants such as overall joint replacement [7]. Meanwhile, biocompatible metals can also be found in orthodontic and dental applications, like dental roots and fillings [8]. This is because these metals can be used without causing any adverse reactions. This is due to the fact that there is no chance of

an allergic response while using these metals. Applications such as vascular stents use shape-memory alloys made of nitinol [9], while magnesium-based improvements on more contemporary alloys are employed for tissue engineering and bone regeneration [10]. Recently, increased research on biocompatible metals has progressed for the non-conventional reconstructive surgery of organs and hard tissue application [11,12]. This study is being done in preparation for the use of these metals. These metals include magnesium-based alloys that increase current alloys' performance, which may be used for tissue engineering and bone regeneration [13,14]. Only a tiny percentage of the alloys and metals that are produced during the manufacturing process are biocompatible and have the potential to be realized in a permanent form as implant materials [15,16]. This is despite the fact that the manufacturing process may create a large range of alloys and metals. The mechanisms used in the vast majority of orthopedic medical equipment can be bought and sold in the commercial market. The most often used kinds of biocompatible metal alloys are stainless steels, cobalt-chromium alloys, titanium and its alloys and titanium. Stainless steel has higher erosion and corrosion resistance [17-27]. Co-Cr alloys have high wear and corrosion resistance as well as have ease of machinability [28-38]. Ti and its alloys hold good wear and corrosion-resistant properties, but their machinability is a quite tough task [4,5,7,39-45]. Y_2O_3, yttria-stabilized-zirconia (YSZ), HAP and ZrO_2 are the most widely used for bio-implant applications [35,46-51].

This research refers to the function of the biocompatible metals used most often in biomedical applications. These metals are considered to be biocompatible. These metals consist of stainless steels, alloys based on cobalt and chromium, titanium and its alloys, and other alloys based on titanium. In addition, the behavior of biocompatible metal alloys, includingtheir biocompatibility and resistance to corrosion, will be researched.

Implant materials

The medical industry's use of biocompatible materials has grown dramatically during the previous two decades. Gold, silver and iron are some of the metals used most often in producing long bone fracture pins and spinal cables. Joint/replacement fractured/damaged bone is the primary use of biocompatible materials in orthopedics. Through examination, these materials are put to use as long-term implants, screws, and pins [52].

It is anticipated that alternative biomaterials will affect major areas of burden, including spinal components, tumor bones, orthopedic joints, and dental components. Hence, it is essential to consider both the mechanical strength and performance. Because the bone is so sensitive to changes in its mechanical properties, even at the microscopic level, implants have the potential to influence cellular responses such as differentiation and mineralization. During bone repair, the mechanical characteristics of the implant materials played a major role and had a significant effect. Combining a material's mechanical strength with its ability to withstand fractures is ideal for transplant materials. In comparison to the other types of materials, the tensile strength of metals is the greatest, followed by polymers and ceramics (except for zirconia). In comparison to ceramics, tensile strength, ductility, and resistance to corrosion are all areas in which metals excel. The metallic biomaterial has several deficiencies that need to be addressed. The most important one is the release of toxic elements from metals during metallic corrosion. Among the most common examples are cobalt alloys, stainless steel alloys, titanium alloys, and several other kinds of metallic biomaterials. Since the 1930s, austenitic stainless steel has been used in around ninety percent of osteosynthesis devices. Both the biocompatibility and the mechanical strength of the material were outstanding attributes. As a result of the outstanding strength-to-weight ratio that CO-based alloys

possess, they are often used in the study of human anatomy. The inclusion of chromium at a concentration of more than 18 percent contributes significantly to both the inherent strength and wear resistance of these materials. Titanium's earliest use was in the 1950s when it was utilized in the aerospace industry. Since then, the material has been modified for human medical implants. T Krupp invented implant-grade stainless steel in 1926. It had 18 % Cr and 8 % Ni and became 18Cr-8Ni (AISI 302). The mechanical properties of some biomaterials are shown in Table 1.

Table 1. *Mechanical properties of biomaterials*

Material	Tensile strength, MPa	Compressive strength, MPa	Fracture toughness, MPa m$^{-1/2}$	Ref.
Bio-glass	42	500	2	[53-57]
Ti	345	250-600	58-68	[7,39,43,44]
Stainless steel	465-950	1000	55-95	[20,51,58,59]
Ti alloys	596-1100	450-1850	40-92	[6,7,39,40,43-45,60]
Alumina	270-500	3000-5000	5-6	[33,34,48,61,62]

In biomedical sectors, commercial-grade stainless steel is utilized to make surgical and dentistry tools. Manufacturing techniques that are specific to stainless steel implants, such as vacuum melting (VM), vacuum arc re-melting (VAR), or electroslag refining (ESR), provide resistance to pitting and crevice corrosion and a reduction in the amount of non-metallic additives. Most people choose austenitic stainless steel because of its versatility. Low cost, high strength and ductility, machinability, and mechanical qualities can be controlled easily. Implants made of vacuum-melted 316L stainless steel are available on the commercial market. Afterward, biomedical industries began employing titanium implants in the 1930s, The titanium alloy plays a great role due to its thermo mechanical properties and its low density. Vacuum processing necessitated a high temperature to avoid the formation of a reaction with oxygen. Pure titanium (Cp-Ti) is the only commercially available form of the four grades.

The present work focuses on these two materials for testing and evaluating their machinability and biocompatibility being an implant material using wire-cut electrical discharge machining (WEDM)approach.

WEDM technique

Machine tools, control systems, power supply units, and dielectric supply units are all included in the WEDM. In addition to the primary worktable, the tool control section includes an auxiliary work table, a wire feed mechanism, and a wire cutter. There is a large worktable on which the pieces of work are placed. 1 μm increments are used in servo motor control of axial movement. The *U* and *V* axes of the table are parallel to the *X* and *Y* axes, resulting in a flat configuration. Continuous feed is ensured by two guides on either side of the wire feed system (in and out). Guides aid in maintaining the wire's tension. Due to the *inactive U-V* axis and lower guide, there is a transverse displacement of the top wire guide. To remove material from a workpiece, an electrical spark is generated by the pulse generator unit. As a dielectric liquid, deionized water was used to keep the top and bottom work pieces hydrated. The low viscosity and rapid cooling speeds of deionized water are its primary advantages. The controller stores the route of the work item and shifts it transversely. Tilting the tapper as the *X-Y* table moves along a specified route and the *U-V* table remains stationary is required for a straight cut. To carry out the operations, the route information is completely controlled by the CNC [8]. Figure 1 given demonstrates the basic principle of WEDM. Based on its principle of working, WEDM produced responses in terms of surface roughness and material removal rate.
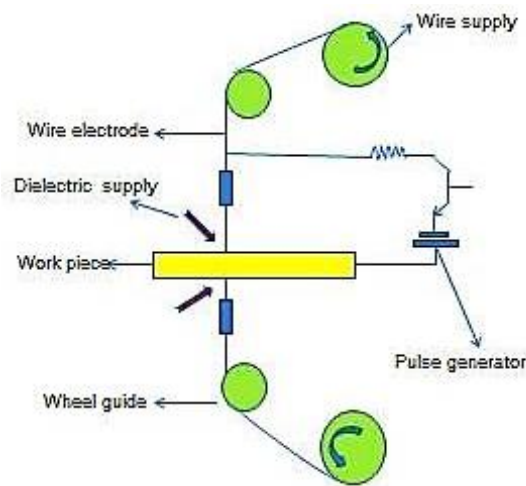
Figure 1. *Schematic diagram of the basic principle of the WEDM process.*

Surface roughness

Over a given length, it may be summed up as a deviation from the nominal surface in the vertical axis. The micro-level profile of a machined surface's key nomenclature is:

- Roughness Distance from the nominal surface to the peak of the waviness.
- The Roughness Width is the distance between the peaks.
- The maximum spacing of irregularities included in the measurement is represented by the cut-off distance/width.
- In machining parlance, the term "lay" refers to the direction in which a surface pattern is generated as a reflection of the machining process.

The roughness average (R_a), sometimes referred to as the arithmetic mean of the precise quantity of each height slightly above the nominal surface, is a metric that may be used to highlight the surface imperfections. R_a is frequently referred to be the arithmetic mean of each height slightly above the nominal surface. Roughness may also be addressed in terms of roughness maximal (R_z), which is the distance between the highest point as well as the lowest point on the surface. This distance is measured from one point on the surface to the next. Similar to how this may be stated in terms of roughness, the roughness could also be described in terms of roughness. Roughness peak (R_p), also known as the maximum height value from the nominal surface, is an additional method that may be used to replicate the surface's roughness. This method is one of several alternative methods [63].

Particularly in the case of the WEDM process, the undulation that is present on the surface of the machined component runs parallel to the direction in which the wire is moving. Because the energy applied to melt the specimen results in the volume lost in the metal, the surface roughness is dependent on the electrical parameters of the machining process, such as the voltage applied between the gaps, the pulse-on time, *etc*.

Material removal rate

Material removal rate(MRR) sometimes referred to as is the amount of material removed in a certain amount of time, with the objective of achieving higher levels of productivity overall. It is recommended that the MRR machining process continue its upward trajectory toward increased productivity without compromising surface quality (*i.e.* decrease in surface quality). High MRR combined with a high-quality surface finish should lead to increased productivity in the component production process. Calculating the MRR of the machining process may be done using either the

length of the machining time or the weight loss approach. Both methods are available. Eqs. (1) and (2) provides a representation of the empirical equation utilized for the calculation of MRR by measuring the amount of time spent cutting throughout the process of machining [64].

MRR = Cutting rate × Width × Depth of work   (1)

Cutting rate = Total machining length / Time of machining   (2)

where, MRR is measured in mm^3 min^{-1}, the cutting rate is in mm/min, and width and depth are in mm. The MRR of the machining process (g min^{-1}) can also be calculated using the weight loss of the specimen, eqs. (3) and (4):

MRR = Weight loss / Machining time   (3)

Weight loss = Weight before machining - Weight after machining   (4)

Experimental

For the purpose of this examination, orthopedic human implant materials that are available for purchase on the market were acquired for the research project. The technical grade of implants that were acquired from literature who served as the primary supplier of the implant material, 48 for orthopedics. For the purpose of this investigation, titanium-based human implant grade T-L107.12 (hole diameter: 4.9 mm; 12 holes) materials were used. Table 1 details the material's nominal chemical composition, which may be obtained by utilizing the data from Table 2.

Table 2. Nominal composition of Ti-based human implant material of grade T-L107.12 implant

Alloying elements	Al	V	C	O	N	Fe	Ti
Content, wt. %	5.5	4.5	0.08	0.13	0.05	0.25	Balance

Figure 2. ELEKTRA wire EDM machine

Wire electrical discharge machining

The WEDM machine, which is computer-aided and numerically controlled, is used in the performance of the experimental research (Model: ELEKTRA). The WEDM machines are made up of the power supply unit, the flushing unit, and the industrial machinery process speed. The definition of the method makes use of deionized water as the dielectric medium, and the electrode wire material is a half-hard EDM brass wire with a diameter of 0.25 millimeters. Figure 2 given shows the EDM machine used in the present work.

Specifications of the equipment

The machine, the control cabinet, and the worktable are the three primary elements of the ELEKTRA wire EDM. In Table 3, the representation of the machine's specifications has been illustrated. Table 3 provides an overview of the input process parameters that may be modified for implant machining. A problem has been constructed using the input variables and the MINITAB program to design twenty-one sets of input parameter combinations for experiments. This problem was built using the input variables.

Table 3. *ELEKTRA wire EDM technical specification*

No.	Parameter	Value
1	Main table traverse ($X \times Y$), mm	300×400
2	Aux. table traverse ($X \times Y$), mm	80×80
3	Table size, mm	440×650
4	Maximum taper angle, °	±30° / 50 mm
5	Maximum workpiece height. mm	200
6	Maximum workpiece weight, kg	300
7	Resolution, µm	0.5
8	Max. JOG speed, mm min^{-1}	900
9	Maximum wire spool capacity, kg	5
10	Wire electrode diameter. mm	0.25 (standard) 0.15, 0.20 (optional)
11	Least input increment, µm	1
12	Interpolation	Linear and circular
13	Connected load, kVA	10
14	Wire tension, g	1600

Experiment design for machining implant material

In Table 4, the data for the experiment design has been given. All conceivable permutations of the machinability assessment are tested in terms of surface roughness (R_a) and material removal rate (MRR). The MITUTOYO roughness meter is used to determine the surface roughness of each machined surface individually (Model: Surftest SJ 410, Japan). In order to compute the material removal rate, use the following mathematical relationship, eq. (5):

MRR, mm^3/min = cutting rate × width × depth of work   (5)

As a consequence of the investigation, the impact of each input process parameter is examined using Minitab software to do the necessary mathematical calculations for the analysis of variance (ANOVA). Based on the data, conclusions were drawn that revealed the best process condition for machining stainless steel implantation materials in terms of surface quality and machinability.

Surface roughness

The values of the surface's two-dimensional roughness may be assessed using a probe-style tester with an MITUTOYO roughness meter (model number: Surface test SJ 410; manufactured in Japan) which is configured in the manner seen in Figure 3. The Ra values show where the peaks and troughs are located in a certain direction parallel to the path taken by the probe. The measures of the surface roughness are as follows:

They are manufactured with a cut-off value of 0.8 mm and thus are manufactured in the opposite direction from that in which the wire traverses, which ultimately results in increased values for the surface's roughness. Vertical moments were able to measure motions to an accuracy of 0.01 mm.

Table 4. Experiment design for machining implant material

Run	Pulse-on, μs	Pulse-on, μs	Voltage, V
I	5	8	65
2	5	3	65
3	5	8	65
4	6	5	80
5	6	10	50
6	3	10	80
7	3	5	80
8	3	10	50
9	5	8	65
10	5	8	40
11	5	8	65
12	2	8	65
13	5	8	90
14	6	5	50
15	3	5	50
16	5	8	65
17	5	8	65
18	5	8	65
19	7	8	65
20	5	I2	65
21	6	10	80

Figure 3. Surface roughness tester

Analysis of variance

The analysis of changes is a computationally based method that quantifies the impact of every input parameter on the overall response. The variation in the data caused by interactions is referred to as the variance within the control factors used in the experiment. These components are what make up the experiment. The F-ratio, also known as Fisher's ratio, is used in order to determine which parameters are the most important and which are the least significant. The results of the ANOVA test reveal which of the factors had the greatest impact on the overall response.

Results and discussion

Machinability of implants

Surface roughness of the WEDM machined implants

Experiments were done using a statistical model that had already been set up, and the measured surface roughness is shown in Table 5.

Table 5. *Surface roughness with reference to individual process parameters involved in machining titanium-based implant material*

Run	Pulse-on, µs	Pulse-off, µs	Voltage, V	R_a / µm
1	6	7	65	3.284
2	6	4	65	2.883
3	6	7	65	2.524
4	5	6	80	2.274
5	5	9	50	3.613
6	4	9	80	2.103
7	4	6	80	2.131
8	4	9	50	2.608
9	6	7	65	2.781
10	6	7	50	3.385
11	6	7	65	2.385
12	3	7	65	1.739
13	6	7	90	1.883
14	5	6	50	3.378
15	4	6	50	3.237
16	7	7	65	2.429
17	7	7	65	2.374
18	7	7	65	2.247
19	9	7	65	2.782
20	7	11	65	2.222
21	7	9	80	2.112

When it comes to surface roughness, the lowest voltage combined with either a pulse-on (T_{on}) or a pulse-on (T_{off}) has the most impact. The linearity goodness of fit (R^2) for the experimental data is 84.61 %, confirming all of this. A linear regression equation for such a suggested model is created utilizing the applied voltage (V) and the T_{on} as the most essential parameters to analyze the theoretical difference in R_a. The regression line's equation (6) is as follows:

$$R_a = 8.6487\ V\ 0.052418\ T_{on}\ \text{-}0.30245 \tag{6}$$

Surface roughness with reference to the applied voltage at three different T_{on} is shown in Figure 4. You may compute the theoretical changes in surface roughness by adjusting the applied voltage and pulse-on time. Surface roughness has a higher order response to diverse applied voltages than pulse-on time.

Material removal rate of the WEDM machined implants

This condition existed, just like the roughness of the surface. The goodness of fit in linearity (R^2) reveals that the experimental data for MRR are as high as 92.5 % based on all of the aforementioned.
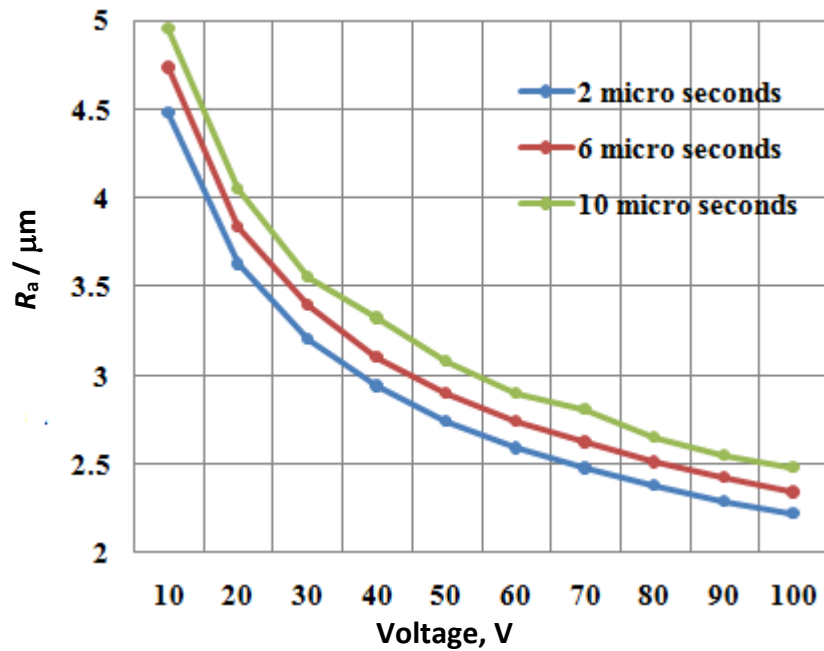
Figure 4. *Theoretical variations in surface roughness with reference to the applied voltage at three different pulses on time*

A linear regression equation for such a suggested model was created by taking into consideration the applied voltage and the pulse-on time to analyze the theoretical difference in MRR (T_{on}). The regression equation is shown in the equation (7):

$$MRR = 0.01164\ V\ 0.236211\ T_{on} - 1.0997 \tag{7}$$

The empirical calculations of the theoretical changes in surface roughness and the rate of material removal are accomplished by adjusting the applied voltage and the pulse-on time. Material removing rate with reference to the applied voltage at three different pulses on time is shown in Figure 5. Convergences are seen in the material removal rate when the voltage is increased to its maximum for a variety of pulse-on times.
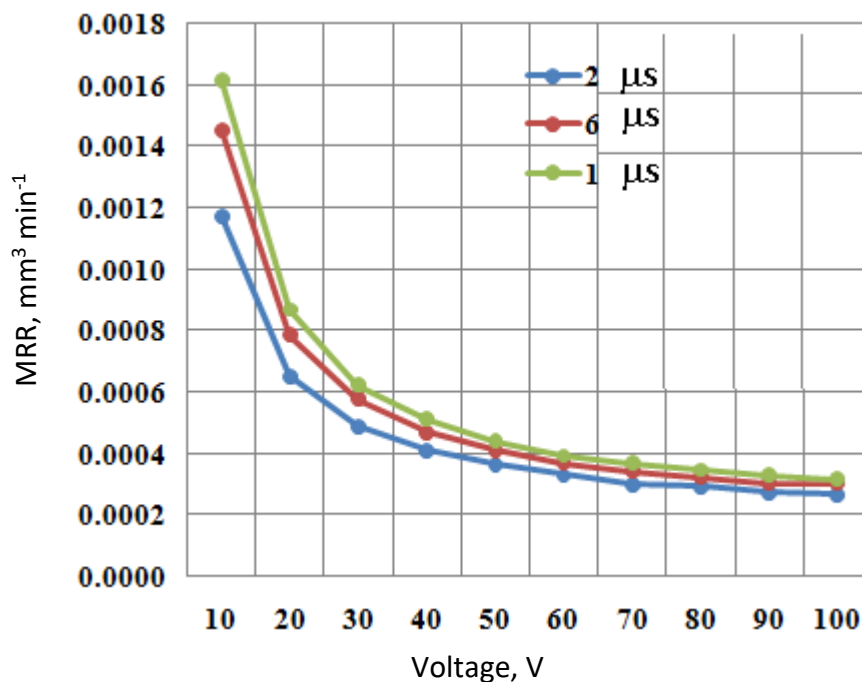

Figure 5. *Theoretical variations in MRR with reference to the applied voltage at three different* T_{on} */ μs*

***Table 6.** Surface roughness with reference to individual process parameters involved in machining titanium-based implant material*

Run	T_{on} / μs	T_{off} / μs	Voltage, V	R_a / μm
1	5	8	65	3.193
2	5	3	65	2.992
3	5	8	65	2.412
4	6	5	80	2.180
5	6	10	50	3.504
6	3	10	80	2.003
7	3	5	80	2.232
8	3	10	50	2.507
9	5	8	65	2.981
10	5	8	50	3.475
11	5	8	65	2.175
12	2	8	65	1.929
13	5	8	90	1.994
14	6	5	50	3.269
15	3	5	50	3.126
16	5	8	65	2.318
17	5	8	65	2.264
18	5	8	65	2.136
19	7	8	65	2.692
20	5	12	65	2.111
21	6	10	80	2.023

Influence of process parameters on surface roughness and material removal rate

Experiments conducted using a preset statistical model are submitted for a thorough examination. Following the conclusion of the inquiry, the experimental data are statistically analyzed to establish the contribution of each individual process parameter and their effect on machining. Table 7 depicts the findings of this investigation.

***Table 7.** Level of process parameters contribution towards surface roughness and material removal rate*

	Contribution, %			
	T_{on}	T_{off}	Voltage	Error
R_a	9.12	0.41	75.11	15.36
MRR	2.36	1.20	88.94	7.50

Calculating the contributions of the process parameters based on the results of an analysis of variance is an empirical approach (ANOVA). Surface roughness and material removal rate are shown in Table 7. The three critical machining parameters for processing titanium-based human implant materials throughout the machining process are applied voltage, pulse-on time, and pulse-on time. T on is another name for pulse-on time. Toff stands for "pulse-on time". Given this data, it is clear that the applied voltage is the most important variable in operation, as it has a significant impact on both the surface polish (75.11 %) and the rate of material removal (88.9 %).

A wire-EDM machining process very similar to the one described above was carried out. Statistical analysis revealed that the voltage provided had a substantial influence on the surface finish produced. When machining is done, the voltage being applied will, in the majority of instances, be directly involved in the formation of resistance as well as plasma arcs (between the wire and the contact zone) between the dielectric medium and the wire. The other two parameters are the management of the

pulse-on time for plasma spark creation and T_{on} surface finish and material removal contributions, respectively. The surface finish contribution of T_{on} is 9 %, and the material removal contribution is 2.3 %. The inaccuracy in the design may be described as a percentage. When that percentage is determined, it comes out to 15 % for the surface finish and 1.5 % for the material removal rate appropriately. The variation in inaccuracy for Ra and MRR is due to the fact that the surface polish does not remain constant in relation to the quantity of material that has been removed. The contribution of process parameters will be directly influenced by the marginal variance obtained while taking the average of Ra for three different sites. SEM surface investigation using micrographs taken by that instrument is carried out so that supporting evidence may be presented. The materials and different processes can be used to process the surface properties [65,66]. Surface qualities may be modified via the use of various materials and techniques [67-72].

Conclusions

The Ra value is measured in micrometers over the machined surface treated with WEDM. When the largest pulse-on setting is utilized and the lowest applied voltage is chosen, it is fair to anticipate that the intensity of the electro-spark needed to machine the material will be reduced. With an increase within the high intensity of electro spark generated, the roughness of the machined surface was revealed to be greater, while quality is discovered to be lower. In addition to the roughness assessment, the same surface is then investigated further using electron imaging and 3D profile surface analysis.

References

[1] D. D. Kiradzhiyska, R. D. Mantcheva, Overview of Biocompatible materials and their use in medicine, *Folia Medica* **61** (2019) 34-40. https://doi.org/10.2478/folmed-2018-0038

[2] K. A. Hing, Bone repair in the twenty-first century: biology, chemistry or engineering? *Philosophical Transactions of the Royal Society A* **362** (2004) 2821-2850 https://doi.org/10.1098/rsta.2004.1466

[3] M. Saini, Implant biomaterials, *World Journal of Clinical Cases* **3** (2015) 52. https://doi.org/10.12998/wjcc.v3.i1.52

[4] C. Prakash, H. K. Kansal, B. Pabla, S. Puri, A. Aggarwal, Electric discharge machining - A potential choice for surface modification of metallic implants for orthopedic applications, *Proceedings of the Institution of Mechanical Engineers B* **230** (2016) 331-353. https://doi.org/10.1177/0954405415579113

[5] C. Prakash, S. Singh, C. Pruncu, V. Mishra, G. Królczyk, D. Pimenov, A. Pramanik, Surface Modification of Ti-6Al-4V Alloy by Electrical Discharge Coating Process Using Partially Sintered Ti-Nb Electrode, *Materials* **12** (2019) 1006. https://doi.org/10.3390/ma12071006

[6] S. Pradhan, S. Singh, C. Prakash, G. Królczyk, A. Pramanik, C.I. Pruncu, Investigation of machining characteristics of hard-to machine Ti-6Al-4V-ELI alloy for biomedical applications, *Journal of Materials Research and Technology* **8** (2019) 4849-4862 https://doi.org/10.1016/j.jmrt.2019.08.033

[7] C. Prakash, H. K. Kansal, B. S. Pabla, S. Puri, Powder Mixed Electric Discharge Machining: An Innovative Surface Modification Technique to Enhance Fatigue Performance and Bioactivity of β-Ti Implant for Orthopedics Application, *Journal of Computing and Information Science in Engineering* **16(4)** (2016) 041006. https://doi.org/10.1115/1.4033901

[8] A. Mandal , A. R. Dixit, A. Kumar Das, N. Mandal, Modeling and Optimization of Machining Nimonic C-263 Super Alloy Using Modeling and Optimization of Machining Nimonic C-263

Superalloy using Multicut Strategy in WEDM, *Materials and Manufacturing Processes* **31(7)** (2015) 860-868. https://doi.org/10.1080/10426914.2015.1048462

[9] C. D. J. Barras, K. A. Myers, Nitinol - Its Use in Vascular Surgery and Other Applications, *European Journal of Vascular and Endovascular Surgery* **19** (2000) 564-569. https://doi.org/10.1053/ejvs.2000.1111s

[10] C. Liu, Z. Ren, Y. Xu, S. Pang, X. Zhao, Y. Zhao, Biodegradable Magnesium Alloys Developed as Bone Repair Materials, *Scanning* **2018** (2018) 9216314. https://doi.org/10.1155/2018/9216314

[11] Y. Ikada, Challenges in tissue engineering, *Journal of The Royal Society Interface* **3** (2006) 589-601. https://doi.org/10.1098/rsif.2006.0124

[12] S. Al-Himdani, Z. M. Jessop, A. Al-Sabah, E. Combellack, A. Ibrahim, S. H. Doak, A. M. Hart, C. W. Archer, C. A. Thornton, I. S. Whitaker, Tissue-Engineered Solutions in Plastic and Reconstructive Surgery: Principles and Practice, *Frontiers in Surgery* **4** (2017) 4. https://doi.org/10.3389/fsurg.2017.00004

[13] S. P. Pilipchuk, A. B. Plonka, A. Monje, A. D. Taut, A. Lanis, B. Kang, W. V. Giannobile, Tissue engineering for bone regeneration and osseointegration in the oral cavity, *Dental Materials* **31** (2015) 317-338. https://doi.org/10.1016/j.dental.2015.01.006

[14] J. M. Kanczler, J. A. Wells, D. M. R. Gibbs, K. M. Marshall, D. K. O. Tang, R. O. C. Oreffo, *Bone tissue engineering and bone regeneration*, in *Principles of Tissue Engineering*, R. Lanza, R. Langer, J. R. Vacanti, A. Atala, Eds., Elsevier, 2020, 917-935. https://doi.org/10.1016/B978-0-12-818422-6.00052-6

[15] K. Moghadasi, M. S. Mohd Isa, M. A. Ariffin, M. Z. Mohd Jamil, S. Raja, B. Wu, M. Yamani, M. R. Bin Muhamad, F. Yusof, M. F. Jamaludin, M.S . bin Ab Karim, B. Binti Abdul Razak, N. bin Yusoff, A review on biomedical implant materials and the effect of friction stir based techniques on their mechanical and tribological properties, *Journal of Materials Research and Technology* **17** (2022) 1054-1121. https://doi.org/10.1016/j.jmrt.2022.01.050

[16] R. Davis, A. Singh, M. J. Jackson, R. T. Coelho, D. Prakash, C. P. Charalambous, W. Ahmed, L. R. R. da Silva, A. A. Lawrence, A comprehensive review on metallic implant biomaterials and their subtractive manufacturing, *The International Journal of Advanced Manufacturing Technology* **120** (2022) 1473-1530. https://doi.org/10.1007/s00170-022-08770-8

[17] J. Singh, J. P. Singh, Performance analysis of erosion resistant Mo2C reinforced WC-CoCr coating for pump impeller with Taguchi's method, *Industrial Lubrication and Tribology* **74** (2022) 431-441. https://doi.org/10.1108/ILT-05-2020-0155

[18] J. Singh, S. K. Mohapatra, S. Kumar, Performance analysis of pump materials employed in bottom ash slurry erosion conditions, *Jurnal Tribologi* **30** (2021) 73-89. https://jurnaltribologi.mytribos.org/v30/JT-30-73-89.pdf

[19] J. Singh, J. P. Singh, Numerical Analysis on Solid Particle Erosion in Elbow of a Slurry Conveying Circuit, *Journal of Pipeline Systems Engineering and Practice* **12** (2021) 04020070. https://doi.org/10.1061/(asce)ps.1949-1204.0000518

[20] J. Singh, A review on mechanisms and testing of wear in slurry pumps, pipeline circuits and hydraulic turbines, *Journal of Tribology* **143** (2021) 0900801. https://doi.org/10.1115/1.4050977

[21] J. Singh, Wear performance analysis and characterization of HVOF deposited Ni-20Cr$_2$O$_3$, Ni-30Al$_2$O$_3$, and Al$_2$O$_3$-13TiO$_2$ coatings, *Applied Surface Science Advances* **6** (2021) 100161. https://doi.org/10.1016/j.apsadv.2021.100161

[22] J. Singh, Slurry erosion performance analysis and characterization of high-velocity oxy-fuel sprayed Ni and Co hardsurfacing alloy coatings, *Journal of King Saud University - Engineering Sciences* (2021). https://doi.org/10.1016/j.jksues.2021.06.009

[23] J. Singh, S. Kumar, S. K. Mohapatra, Study on Solid Particle Erosion of Pump Materials by Fly Ash Slurry using Taguchi's Orthogonal Array, *Tribologia - Finnish Journal of Tribology* **38** (2021) 31-38. https://doi.org/10.30678/fjt.97530

[24] J. Singh, Tribo-performance analysis of HVOF sprayed 86WC-10Co$_4$Cr and Ni-Cr$_2$O$_3$ on AISI 316L steel using DOE-ANN methodology, *Industrial Lubrication and Tribology* **73** (2021) 727-735. https://doi.org/10.1108/ILT-04-2020-0147

[25] J. Singh, S. Singh, Neural network prediction of slurry erosion of heavy-duty pump impeller/casing materials 18Cr-8Ni, 16Cr-10Ni-2Mo, super duplex 24Cr-6Ni-3Mo-N, and grey cast iron, *Wear* **476** (2021) 203741. https://doi.org/10.1016/j.wear.2021.203741

[26] J. Singh, *Application of Thermal Spray Coatings for Protection against Erosion, Abrasion, and Corrosion in Hydropower Plants and Offshore Industry*, in *Thermal Spray Coatings*, L. Thakur, H. Vasudev, Eds., Taylor and Francis Inc. CRC Press, Florida, 2021, 243-284. https://doi.org/10.1201/9781003213185-10

[27] J. Singh, S. Singh, J. Pal Singh, Investigation on wall thickness reduction of hydropower pipeline underwent to erosion-corrosion process, *Engineering Failure Analysis* **127** (2021) 105504. https://doi.org/10.1016/j.engfailanal.2021.105504

[28] H. Vasudev, L. Thakur, H. Singh, A. Bansal, A study on processing and hot corrosion behaviour of HVOF sprayed Inconel718-nano Al$_2$O$_3$ coatings, *Materials Today Communications* **25** (2020) 101626. https://doi.org/10.1016/j.mtcomm.2020.101626

[29] H. Vasudev, L. Thakur, H. Singh, A. Bansal, An investigation on oxidation behaviour of high velocity oxy-fuel sprayed Inconel718-Al$_2$O$_3$ composite coatings, *Surface and Coatings Technology* **393** (2020) 125770. https://doi.org/10.1016/j.surfcoat.2020.125770

[30] H. Vasudev, G. Singh, A. Bansal, S. Vardhan, L. Thakur, Microwave heating and its applications in surface engineering, *Materials Research Express* **6** (2019) 102001. https://doi.org/10.1088/2053-1591/ab3674

[31] G. Singh, H. Vasudev, A. Bansal, S. Vardhan, S. Sharma, Microwave cladding of Inconel-625 on mild steel substrate for corrosion protection, *Materials Research Express* **7(2)** (2020) 026512. https://doi.org/10.1088/2053-1591/ab6fa3

[32] H. Vasudev, L. Thakur, H. Singh, A. Bansal, Mechanical and microstructural behaviour of wear resistant coatings on cast iron lathe machine beds and slides, *Kovove Materialy* **56(1)** (2018) 55-63. https://doi.org/10.4149/km2018-1-55

[33] G. Prashar, H. Vasudev, Á. S. A. Gra, Structure - Property Correlation of Plasma-Sprayed Inconel625- Al$_2$O$_3$ Bimodal Composite Coatings for High-Temperature Oxidation Protection, *Journal of Thermal Spray Technology* (2022). https://doi.org/10.1007/s11666-022-01466-1

[34] H. Vasudev, G. Prashar, L. Thakur, A. Bansal, electrochemical corrosion behavior and microstructural characterization of HVOF sprayed inconel718-Al$_2$O$_3$ composite coatings, *Surface Review and Letters* **29** (2022) 2250017. https://doi.org/10.1142/S0218625X22500172

[35] P. Singh, A. Bansal, H. Vasudev, In situ surface modification of stainless steel with hydroxyapatite using microwave heating, *Surface Topography: Metrology and Properties* **9** (2021) 35053. https://doi.org/10.1088/2051-672X/ac28a9

[36] V. Dutta, L. Thakur, B. Singh, H. Vasudev, A Study of Erosion - Corrosion Behaviour of Friction Stir-processed Chromium-reinforced NiAl Bronze Composite, *Materials* **15** (2022) 5401. https://doi.org/doi.org/10.3390/ma15155401

[37] G. Prashar, H. Vasudev, In fl uence of heat treatment on surface properties of HVOF deposited WC and Ni-based powder coatings, *Surface Topography: Metrology and Properties* **9** (2021) 43002. https://doi.org/10.1088/2051-672X/ac3a52

[38] G. Prashar, H. Vasudev, parameters and heat treatment on the corrosion performance of Ni-based, *Surface Review and Letters* **29** (2022) 2230001. https://doi.org/10.1142/S0218625X22300015.

[39] C. Prakash, M. S. Uddin, Surface modification of β-phase Ti implant by hydroaxyapatite mixed electric discharge machining to enhance the corrosion resistance and in-vitro bioactivity, *Surface and Coatings Technology* **326** (2017) 134-145. https://doi.org/10.1016/j.surfcoat.2017.07.040

[40] S. Pradhan, S. Singh, C. Prakash, G. Królczyk, A. Pramanik, C. I. Pruncu, Investigation of machining characteristics of hard-to-machine Ti-6Al-4V-ELI alloy for biomedical applications, *Journal of Materials Research and Technology* **8** (2019) 4849-4862. https://doi.org/10.1016/j.jmrt.2019.08.033

[41] C. Prakash, S. Singh, M. Singh, K. Verma, B. Chaudhary, S. Singh, Multi-objective particle swarm optimization of EDM parameters to deposit HA-coating on biodegradable Mg-alloy, *Vacuum* **158** (2018) 180-190. https://doi.org/10.1016/j.vacuum.2018.09.050

[42] C. Prakash, S. Singh, B. S. Pabla, M. S. Uddin, Synthesis, characterization, corrosion and bioactivity investigation of nano-HA coating deposited on biodegradable Mg-Zn-Mn alloy, *Surface and Coatings Technology* **346** (2018) 9-18. https://doi.org/10.1016/j.surfcoat.2018.04.035

[43] C. Prakash, H. K. Kansal, B. S. Pabla, S. Puri, Multi-objective optimization of powder mixed electric discharge machining parameters for fabrication of biocompatible layer on β-Ti alloy using NSGA-II coupled with Taguchi based response surface methodology, *Journal of Mechanical Science and Technology* **30** (2016) 4195-4204. https://doi.org/10.1007/s12206-016-0831-0

[44] C. Prakash, H.K. Kansal, B.S. Pabla, S. Puri, Processing and Characterization of Novel Biomimetic Nanoporous Bioceramic Surface on β-Ti Implant by Powder Mixed Electric Discharge Machining, *Journal of Materials Engineering and Performance* **24** (2015) 3622-3633. https://doi.org/10.1007/s11665-015-1619-6

[45] C. Prakash, H. K. Kansal, B. S. Pabla, S. Puri, Experimental investigations in powder mixed electric discharge machining of Ti-35Nb-7Ta-5Zrβ-titanium alloy, *Materials and Manufacturing Processes* **32** (2017) 274-285. https://doi.org/10.1080/10426914.2016.1198018

[46] P. Singh, H. Vasudev, A. Bansal, Effect of post-heat treatment on the microstructural , mechanical , and bioactivity behavior of the microwave- assisted alumina-reinforced hydroxyapatite cladding, *Proceedings of the Institution of Mechanical Engineers, Part E: Journal of Process Mechanical Engineering* (2022) https://doi.org/10.1177/09544089221116168

[47] G. Prashar, H. Vasudev, D. Bhuddhi, Additive manufacturing: expanding 3D printing horizon in industry 4.0, *International Journal on Interactive Design and Manufacturing* (2022) https://doi.org/10.1007/s12008-022-00956-4

[48] G. Prashar, H. Vasudev, High temperature erosion behavior of plasma sprayed Al2O3 coating on AISI-304 stainless steel, *World Journal of Engineering* **18** (2020) 760-766. https://doi.org/10.1108/WJE-10-2020-0476

[49] J. Singh, S. Singh, Neural network supported study on erosive wear performance analysis of Y2O3/WC-10Co4Cr HVOF coating, *Journal of King Saud University - Engineering Sciences* (2022). https://doi.org/10.1016/j.jksues.2021.12.005

[50] J. Singh, S. Kumar, S. K. Mohapatra, An erosion and corrosion study on thermally sprayed WC-Co-Cr powder synergized with Mo2C/Y2O3/ZrO2 feedstock powders, *Wear* **438**-**439** (2019) 102751. https://doi.org/10.1016/j.wear.2019.01.082

[51] J. Singh, S. Singh, R. Gill, Applications of biopolymer coatings in biomedical engineering, *Journal of Electrochemical Science and Engineering* (2022). https://doi.org/10.5599/jese.1460

[52] D. Lacroix, *3 - Biomechanical aspects of bone repair*, Elsevier Ltd, 2019. https://doi.org/10.1016/B978-0-08-102451-5.00003-2

[53] S. M. Fathy, M. V. Swain, In-vitro wear of natural tooth surface opposed with zirconia reinforced lithium silicate glass ceramic after accelerated ageing, *Dental Materials* **34** (2018) 551-559. https://doi.org/10.1016/j.dental.2017.12.010

[54] J. Singh, M. Kumar, S. Kumar, S. K. Mohapatra, Properties of Glass-Fiber Hybrid Composites : A Review Properties of Glass-Fiber Hybrid Composites, *Polymer-Plastics Technology and Engineering* **56** (2017) 455-469. https://doi.org/10.1080/03602559.2016.1233271

[55] J. Singh, S. Singh, Materials Science and Engineering B A review on Machine learning aspect in physics and mechanics of glasses, *Materials Science and Engineering B* **284** (2022) 115858. https://doi.org/10.1016/j.mseb.2022.115858

[56] J. Du, *Challenges in Molecular Dynamics Simulations ofMulticomponent Oxide Glasses*, in *Molecular Simulations of Disordered Materials*, C. Massobrio, J. Du, M. Bernasconi, P. S. Salmon, Eds., Springer S, Springer International Publishing AG Switzerland, 2015, 157-180. https://doi.org/10.1007/978-3-319-15675-0-7

[57] D. S. Brauer, C. Rüssel, J. Kraft, Solubility of glasses in the system P_2O_5-CaO-MgO-Na_2O-TiO_2: Experimental and modeling using artificial neural networks, *Journal of Non-Crystalline Solids* **353** (2007) 263-270. https://doi.org/10.1016/j.jnoncrysol.2006.12.005

[58] J. Singh, S. Kumar, G. Singh, Taguchi ' s Approach For Optimization Of Tribo-Resistance Parameters For SS304, *Materials Today: Proceedings* **5** (2018) 5031-5038. https://doi.org/10.1016/j.matpr.2017.12.081

[59] J. Singh, S. Kumar, S. K. Mohapatra, Optimization of Erosion Wear Influencing Parameters of HVOF Sprayed Pumping Material for Coal-Water Slurry, *Materials Today: Proceedings* **5** (2018) 23789-23795. https://doi.org/10.1016/j.matpr.2018.10.170

[60] A. Pramanik, A. K. Basak, G. Littlefair, S. Debnath, C. Prakash, M. A. Singh, D. Marla, R. K. Singh, Methods and variables in electrical discharge machining of titanium alloy, *Heliyon* **6** (2020) e05554. https://doi.org/10.1016/j.heliyon.2020.e05554

[61] H. Vasudev, L. Thakur, H. Singh, A. Bansal, Effect of addition of Al_2O_3 on the high-temperature solid particle erosion behaviour of HVOF sprayed Inconel-718 coatings, *Materials Today Communications* **30** (2022) 103017. https://doi.org/10.1016/j.mtcomm.2021.103017

[62] H. Vasudev, L. Thakur, H. Singh, A. Bansal, Erosion behaviour of HVOF sprayed Alloy718-nano Al_2O_3 composite coatings on grey cast iron at elevated temperature conditions, *Surface Topography: Metrology and Properties* **9** (2021) 035022. https://doi.org/10.1088/2051-672X/ac1c80

[63] K. P. Maity, M. Choubey, K. P. Maity, M. Choubey, *Surface Review and Letters* **26(5)** (2018) 1830008. https://doi.org/10.1142/S0218625X18300083

[64] H. Bisaria, P. Shandilya, Study on crater depth during material removal in WEDC of Ni - rich nickel - titanium shape memory alloy, *Journal of the Brazilian Society of Mechanical Sciences and Engineering* **41** (2019) 157. https://doi.org/10.1007/s40430-019-1655-5

[65] H. Vasudev, Electrochemical Corrosion Behavior and Microstructural Characterization of HVOF Sprayed Inconel-718 Coating on Gray Cast Iron, *Journal of Failure Analysis and Prevention* **21** (2021) 250-260. https://doi.org/10.1007/s11668-020-01057-8

[66] M. Singh, H. Vasudev, R. Kumar, Corrosion and tribological behaviour of bn thin films deposited using magnetron sputtering, *International Journal of Surface Engineering and*

Interdisciplinary Materials Science **9** (2021) 24-39. https://doi.org/10.4018/IJSEIMS.2021070102

[67] G. Prashar, H. Vasudev, Hot corrosion behavior of super alloys, *Materials Today: Proceedings* **26** (2019) 1131-1135. https://doi.org/10.1016/j.matpr.2020.02.226

[68] A. Mehta, H. Vasudev, S. Singh, Recent developments in the designing of deposition of thermal barrier coatings, *Materials Today: Proceedings* **26** (2020) 1336-1342. https://doi.org/10.1016/j.matpr.2020.02.271

[69] M. Singh, H. Vasudev, R. Kumar, Microstructural characterization of BN thin films using RF magnetron sputtering method, *Materials Today: Proceedings* **26** (2020) 2277-2282. https://doi.org/10.1016/j.matpr.2020.02.493

[70] J. Singh, H. Vasudev, S. Singh, Performance of different coating materials against high temperature oxidation in boiler tubes - A review, *Materials Today: Proceedings* **26** (2020) 972-978. https://doi.org/10.1016/j.matpr.2020.01.156

[71] H. Arora, V. Kumar, C. Prakash, D. Pimenov, M. Singh, H. Vasudev, V. Singh, Analysis of sensitization in austenitic stainless steel-welded joint, *Lecture Notes in Mechanical Engineering* (2021) 13-23. https://doi.org/10.1007/978-981-15-5151-2_2

[72] G. Prashar, H. Vasudev, Structure-property correlation and high-temperature erosion performance of Inconel625-Al_2O_3 plasma-sprayed bimodal composite coatings, *Surface and Coatings Technology* **439** (2022) 128450. https://doi.org/10.1016/j.surfcoat.2022.128450